During the first Jupiter viewing period emissions from the planet were observed in both the hydrogen and helium channels but the data obtained during the second viewing period suffered degradation due to the energetic radiation belt particles. The preliminary estimate of the hydrogen Lyman-α intensity is somewhat less than 1000 rayleighs (*3*) while that of the He emission is approximately 10 to 20 rayleighs. Helium emissions have not previously been observed from Jupiter although the presence of He has been speculated on for many years.

The present Lyman-α measurements are lower than the sounding rocket observations of Rottman *et al.* (*4*). This discrepancy may be partially due to variations in the solar Lyman-α flux, differences in atmospheric properties which depend on solar activity, and calibration uncertainties.

Ultraviolet emissions were also observed in the hydrogen channel from the innermost Galilean satellite Io (JI). It is reasonable to assume that these emissions correspond to Lyman-α since the surface of Io is thought to consist of hydrogen-bearing ices of NH_3 and H_2O (*5*). The atomic hydrogen could result from photolysis and particle bombardment of the atmosphere and surface. If H Lyman-α is the main contributor, the source brightness is approximately 10,000 rayleighs. Such an intensity would seem to require an excitation mechanism in addition to resonance scattering. Aurora-like activity, as produced by energetic electrons accelerated toward Io by its motional electromotive force (*6*), seems an attractive possibility.

Finally, hydrogen channel signals were observed from the equatorial plane of Jupiter during periods when neither the planet nor its satellites were in the field of view. These emissions of several hundred rayleighs in intensity are tentatively interpreted as due to a toroidal cloud of neutral hydrogen in orbit around Jupiter, similar to the hydrogen torus proposed by McDonough and Brice (*7*) for Saturn and Jupiter (*8*). Preliminary analysis indicates that this gas cloud occurs at approximately the orbit of Io, suggesting that this satellite is the source.

DARRELL L. JUDGE
ROBERT W. CARLSON
Department of Physics,
University of Southern California,
Los Angeles 90007

References and Notes

1. The instrument was built at the Analog Technology Corp., Pasadena, Calif., under the supervision of D. Willingham. The liaison with Ames Research Center and the spacecraft interface were handled by T. Wong and R. Tworowski.
2. R. W. Carlson and D. L. Judge, *Planet. Space Sci.* **19**, 327 (1971).
3. One rayleigh corresponds to a column excitation rate of 10^6 photons cm^{-2} sec^{-1}.
4. G. J. Rottman, H. W. Moos, C. S. Freer, *Astrophys. J.* **184**, L89 (1973).
5. T. V. Johnson and T. B. McCord, *Icarus* **13**, 37 (1972).
6. P. Goldreich and D. Lynden-Bell, *Astrophys. J.* **156**, 59 (1969).
7. T. R. McDonough and N. M. Brice, *Icarus* **20**, 136 (1973).
8. ———, private communication, July 1973.

21 December 1973

The Imaging Photopolarimeter Experiment on Pioneer 10

Abstract. *A 2.5-centimeter telescope aboard Pioneer 10 is capable of making two-dimensional spin-scan maps of intensity and polarization in red and blue light at high spatial resolution. During the recent flyby of Jupiter, a large quantity of imaging and polarimetric data was obtained on Jupiter and the Galilean satellites over a wide range of phase angles.*

A prime objective of the encounter phase of our experiment was to gather photometric and polarimetric data on Jupiter over a wide range of phase angles from which the gas abundance above the Jovian clouds and the size, shape, and refractive index of the cloud particles might be derived. In addition, polarimetric observations of the Jovian satellites were sought for comparison with laboratory data. Finally, our intensity data could be displayed as

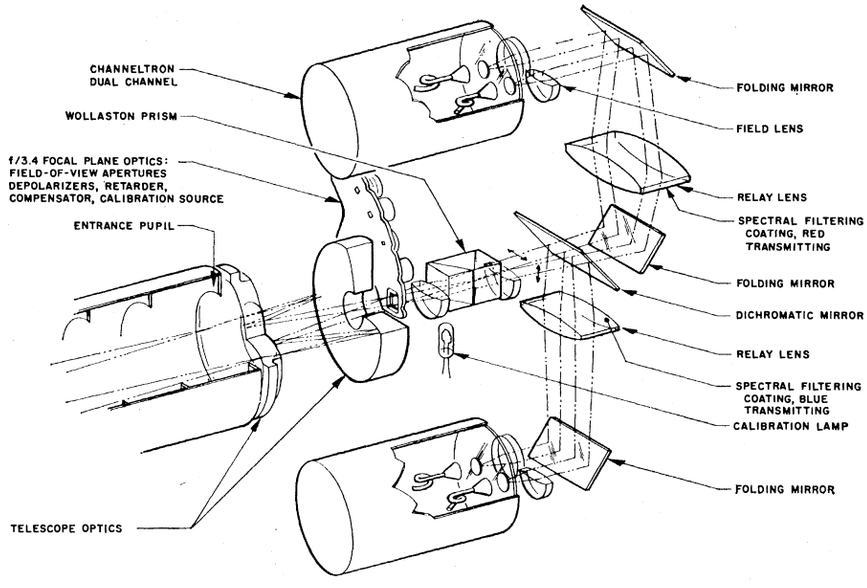

Fig. 1. Optical system of the Pioneer 10 Jupiter imaging photopolarimeter. Light is analyzed into orthogonally polarized beams at two wavelengths (red and blue).

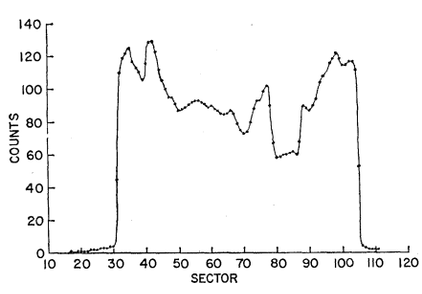

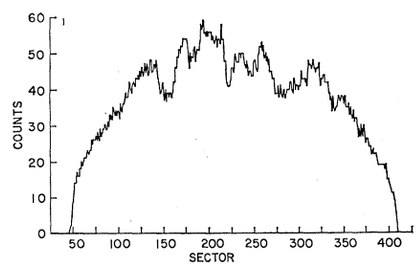

Fig. 2 (left). Scan line on Jupiter taken at 3 R_J in the photopolarimetry mode. The depolarized blue intensity is shown at phase angle $\sim 104°$. Fig. 3 (right). Scan line on Jupiter taken at 35 R_J in the imaging mode. The depolarized red intensity is shown at phase angle $\sim 27°$

images, many of which would have resolution better than that available from the ground.

The imaging photopolarimeter consists of the following: (i) a pointable telescope of 2.5-cm aperture, (ii) a wheel containing focal plane diaphragms and calibration devices, (iii) an optical system to analyze polarization and to split the light into blue and red colors, (iv) Channeltron detectors, and (v) miniaturized logic electronics. The instrument specifications are summarized in Table 1; the optical system is illustrated in Fig. 1. The principles of the design were developed at the University of Arizona and tested on high-altitude balloons, and the instruments for the Pioneer flights were designed and built at the Santa Barbara Research Center (*1*).

The largest focal plane diaphragm, 2.3° by 2.3°, is being used by our coinvestigators at the State University of New York for the study of the zodiacal light (*2*). Next in size is the 0.5° by 0.5° diaphragm which is used in studies of the photometry and polarimetry of Jupiter and its satellites. During the interplanetary cruise, Jupiter was observed regularly in order to watch for possible "rainbow" effects, which are a function of the phase angle and are characteristic for spherical aerosol particles (*3*). The smallest aperture, 0.03° by 0.03°, is used for spin-scan imaging (*4*).

A sequence of some 15,000 commands was generated to control the instrument mode, telescope stepping, data sampling, and gain during the 2 months of encounter observations. These commands were merged with the other spacecraft commands and stored as disk files for transmission in real time. Despite the very large number of critically timed commands, essentially no data were lost as a result of the loss of command capability or the transmission of incorrect commands.

During the period from pericenter (− 7 hours) to + 40 hours, the instrument exhibited several uncommanded changes in the contents of its logic storage registers (probably due to irradiation). Because the round trip travel time of light was 92 minutes, these changes caused the loss of one image and one polarization measurement before pericenter, and four images and three polarization measurements after pericenter. In addition, uncommanded gain decrements caused the loss of two other images before pericenter.

Nevertheless, four polarization maps of the disk at phase angles from 43° to 158° and two images of Jupiter were obtained at ranges between 3 and 7 Jupiter radii (R_J) from the center of the planet (see Table 2). Further, the passage through the Jovian radiation environment seems to have caused no permanent degradation of the instrument. Indeed, even at the peak of the radiation belts, the background never rose to more than 5 percent of the signal in either mode.

One scan line of photopolarimetry data is shown in Fig. 2. Only the depolarized intensity is given here. Note that the brightness varies by more than

Table 1. Imaging photopolarimeter specifications.

Modes of operation	1, Standby 2, Zodiacal light 3, Photopolarimetry 4, Imaging	
Telescope	Maksutov type, 2.5-cm aperture, 8.6-cm focal length	
Spectral bands	Blue, 390 to 500 nm; red, 595 to 720 nm	
Polarization analyzer	Symmetrical Wollaston prism and half-wave retardation plate	
Calibration	Solar diffuser, tungsten lamp, phosphor source, Lyot depolarizer	
Detectors	Two Bendix dual-Channeltrons	
Commands	Three mode initiate, four telescope step control, four data sampling control, two gain control	
Physical properties	18 by 19 by 47 cm, 4.2 kg, 2.2 watts	
	Mode 3 (photopolarimetry)	Mode 4 (imaging)
Instantaneous field of view	8 mrad (0.5°) square	0.5 mrad (0.03°) square
Look angle step (forward-step, backstep, or step inhibit)	8 mrad every four rolls	0.5 mrad every roll
Sampling (spin period = 12.6 seconds)	70° of roll	14° (or 29°) of roll
Analog/digital conversion	Four channels 10 bits each, after each 16-msec integration	Two channels 6 bits each, alternate channels every 0.5 (or 1.0) msec

Table 2. Imaging photopolarimeter encounter observations.

Time	Target*	Range R_J	Phase (deg)	Mode†
−28 days to	Jupiter	350–106	38– 35	3, 4 ‡
− 7 days	JI–JIV	350–106	44– 35	3 §
− 7 days to	Jupiter	106– 23	35– 21	3, 4 ‖
−1 day	JI–JIV	106– 23	20– 62	3 §
−23 hours	JIV	20	98	3
−22 hours	JIV	20	99	4 (2 images)
−21 hours	JIII	11	34	4
−20 to −8 hours	Jupiter	19– 10	19– 12	4 (19 images)
− 7.5 hours	JII	4.5	84	4
− 3 hours	Jupiter	5	43	3
− 1.5 hours	Jupiter	3.5	74	4
− 0.5 hour	Jupiter	3	104	3
+ 0.5 hour	Jupiter	3	141	3
4.5 hours	Jupiter	6	158	3
13.5 hours	Jupiter	14	124	4
14.5 hours	Jupiter	15	123	4
16 hours	Jupiter	16	122	3 (partial map)
19 to 24 hours	Jupiter	19– 22	118–114	4 (6 images)
+ 1 day to	Jupiter	23–106	99– 97	3, 4 ‖
+7 days	JI–JIV	23–106	108– 84	3 §
+ 7 days to	Jupiter	106–350	99– 97	3, 4 ‡
+28 days	JI–JIV	106–350	106– 97	3 §

* JI = Io; JII = Europa; JIII = Ganymede; JIV = Callisto. † Mode 3 is polarimetry mode; instantaneous field of view = 8 mrad. Mode 4 is imaging mode; instantaneous field of view = 0.5 mrad. ‡ Mode 3 followed by several images once per day. § JI–JIV each several times at various phase angles within this range. ‖ Mode 3, 3 hour/day; mode 4, 14 hour/day.

Fig. 4. Blue image taken at 36 R_J at phase angle $\sim 28°$. Note especially the bright spots ringed by dark regions and the many wave structures. The shadow of Io is seen.

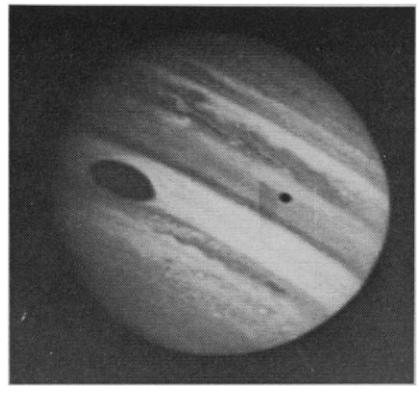

a factor of 2. For each of the 75 sectors on the planet we have accurate measurements of the linear polarization and the direction of vibration. At this wavelength and phase angle the polarization varies from several percent at the center of the disk (viewed normally) to $\sim$ 40 percent at the poles (viewed at grazing angles). These high polarizations result from Rayleigh scattering and will permit a solution for the amount of gas above the cloud tops.

One scan line of red imaging data is shown in Fig. 3. The full gray scale in mode 4 is from 0 to 63. The break in the slope of the curve, particularly obvious at the left of Fig. 3, corresponds to the limb and indicates the high spatial resolution of the data. The noise per pixel is about one count when the signal is 50 counts. Averaging over many pixels is expected to yield relative photometric data of high quality in the blue and red passbands.

An example of the mode 4 blue data displayed as an image is given in Fig. 4. An algorithm has been developed for adding green based on the relative amounts of red and blue in order to produce color images consistent with ground-based experience with Jovian color balance. Since the scan lines are not straight lines on the planet, geometric rectification is done prior to display. The image shows the shadow of Io and a wealth of cloud structure on a variety of scales. The equatorial and polar regions seem much more longitudinally uniform than the mid-latitude regions, which are very structured. Four small bright spots, each about 4000 km in diameter and surrounded by rings of darker material, appear in the south temperate latitudes. North tropical latitudes contain several bright swirls of high contrast, at scales down to the limit of resolution. The low-latitude boundaries of the bright North Tropical Zone and South Temperate Zone exhibit a striking wave pattern. The Red Spot appears not quite oval but has the suggestion of sharp tips at its eastern and western ends. Its border is sharp to the limit of resolution and is somewhat darker than the material it encloses. About 80 images were obtained at resolution up to six times greater than that in this image. In addition, several hundred images were taken during the 2 weeks when the planet was more than 40 resolution elements in diameter, as outlined in Table 2.

We plan several types of studies based on the large volume of data obtained during the flyby. The imaging data will first be rectified and displayed as images for a preliminary cloud morphology classification. The intensities, colors, and polarizations of selected regions observed under different scattering geometries will then be compared with the values computed for various multiple-scattering models. Finally, the photometric and polarimetric data on the Jovian satellites will be compared with laboratory data and ground-based measurements.

T. GEHRELS, D. COFFEEN
M. TOMASKO, L. DOOSE
W. SWINDELL, N. CASTILLO
J. KENDALL, A. CLEMENTS
J. HÄMEEN-ANTTILA, C. KEN KNIGHT
C. BLENMAN, R. BAKER
G. BEST, L. BAKER
University of Arizona, Tucson 85721

References and Notes

1. S. F. Pellicori, E. E. Russell, L. A. Watts, *Appl. Opt.* **12**, 1246 (1973).
2 J. L. Weinberg, M. S. Hanner, H. M. Mann, P. B. Hutchison, R. Fimmel, in *Space Research 13*, A. C. Strickland, Ed. (Akademie-Verlag, Berlin, 1973), p. 1187.
3. A review of the field of polarization studies in planetary atmospheres is given by D. L. Coffeen and J. E. Hansen [in *Planets, Stars, and Nebulae Studied with Photopolarimetry*, T. Gehrels, Ed. (Univ. of Arizona Press, Tucson, 1973)].
4. Various examples of spin-scan imaging are compared by T. Gehrels, V. Suomi, and R. J. Krauss [*Space Research 12*, A. C. Strickland, Ed. (Akademie-Verlag, Berlin, 1972), p. 1765].
5. We are deeply grateful to the large group of people from NASA's Ames Research Center, Jet Propulsion Laboratory, and the Deep Space Net for their combined efforts which resulted in the near-perfect execution of the sequence of some 15,000 instrument commands during November and December 1973. We particularly thank R. Fimmel of Ames Research Center for having personally checked so many of our commands.

21 December 1973

Particle Concentration in the Asteroid Belt from Pioneer 10

Abstract. *The spatial concentration and size distribution for particles measured by the asteroid/meteoroid detector on Pioneer 10 between 2 and 3.5 astronomical units are presented. The size distribution is from about 35 micrometers to 10 centimeters. The exponent of the size dependence varies from approximately −1.7 for the smallest to approximately −3.0 for the largest size measured.*

The asteroid/meteoroid detector being carried on Pioneer 10 and Pioneer 11 measures the contribution to sky brightness in white light from the aggregate of particles in the field of view and the light from bright individual particles which pass through the field of view. The instrument consists of four optical telescopes with 20-cm apertures which look out at an angle of 45° with respect to the spin axis of the spacecraft. The telescopes have 7.5° fields of view and are aligned approximately parallel. The telescopes use RCA 7151 Q photomultipliers with S20 photocathodes. The spectral response is modified by two gold reflections in the Cassegrain-type telescope.

The data obtained from the experiment on Pioneer 10 have been analyzed for the spatial concentration and size distributions of particles observed between 2 and 3.5 A.U. An average result for the 123 particles observed is shown in Fig. 1. This is a cumulative distribution (that is, it is for a given size and larger). The data are generally grouped in the thirds of size decades. However, the entire decade of smallest sizes is grouped together due to the distortion that occurs within 10 m of the telescope. The data points are plotted at the logarithmic mean with a horizontal bar showing the approximate size domain included. Following Dohnanyi (*1*) we have assumed a geometric albedo of 0.2 to derive the particle size. The vertical bars were